Quantitative determination of H_2, HD, and D_2 internal-state distributions by (2+1) resonance-enhanced multiphoton ionization

Klaus-Dieter Rinnen,[a] Mark A. Buntine, Dahv A. V. Kliner, and Richard N. Zare
Department of Chemistry, Stanford University, Stanford, California 94305

Winifred M. Huo
NASA Ames Research Center, Moffett Field, California 94035

(Received 25 January 1991; accepted 26 March 1991)

The relationship between quantum-state populations and ion signals in (2 + 1) resonance-enhanced multiphoton ionization (REMPI) detection of H_2, HD, and D_2 via the $E, F\,^1\Sigma_g^+$ ($v'_E = 0$, $J' = J''$)–$X\,^1\Sigma_g^+$ (v'',J'') transition is determined by calibration against a thermal effusive source. Correction factors are obtained for 102 rovibrational levels for $v'' = 0$, 1, and 2 and J'' ranging from 0 to 17. Within a given v'', rotational correction factors are nearly unity except for the highest J'' levels. The vibrational correction factors vary with v''; (2 + 1) REMPI detection is 2–3 times more sensitive to $v'' = 1$ and 2 than to $v'' = 0$. Experimental correction factors are compared with those derived from a theoretical calculation of the two-photon transition moments by Huo *et al.* [J. Chem. Phys. **95**, 205 (1991)]. In general, the agreement is excellent, which suggests that theoretical correction factors may be used when experimental ones are unavailable.

I. INTRODUCTION

Determination of the internal-state distribution of molecular hydrogen poses a severe experimental challenge because H_2, HD, and D_2 are essentially transparent gases in the infrared, visible, and uv portions of the electromagnetic spectrum. Indeed, the lowest-lying electronic state that is connected to the ground state by an electric-dipole-allowed transition is located at more than 90 000 cm^{-1} (11.2 eV) above the ground state. Consequently, strategies for detecting molecular hydrogen in a quantum-state-specific manner have concentrated on coherent anti-Stokes Raman spectroscopy (CARS),[1-6] laser-induced fluorescence (LIF) with tunable vacuum uv light sources,[7-10] and resonance-enhanced multiphoton ionization (REMPI).[11-13] Of these, REMPI is expected to be most sensitive at low hydrogen concentrations in small probe volumes because of its efficiency in collecting and counting charged particles.

A (2 + 1) REMPI detection scheme for molecular hydrogen has been developed[11] and exploited to determine relative population distributions from gas-phase[14-18] or surface[19] reactions. In this scheme (Fig. 1), absorption of two photons of ~215 nm wavelength induces molecular hydrogen to undergo a Q-branch ($\Delta J = 0$) transition from the (v'',J'') rovibrational level of the $X\,^1\Sigma_g^+$ ground state to the ($v'_E = 0, J' = J''$) rovibrational level of the $E, F\,^1\Sigma_g^+$ state, where $v'_E = 0$ denotes the lowest vibrational level of the inner well of the double-minimum E, F state.[20] The electronically excited molecules are subsequently ionized by absorption of an additional photon from the same laser pulse.

We present here an experimental study of this (2 + 1) REMPI detection process in which we examine the relationship between ion signals and quantum-state populations. We used an effusive beam of H_2, HD, or D_2 in thermal equilibrium with a heated nozzle source at a known temperature (273–1820 K) to calibrate the detection method. Correction factors are derived that relate ion signals to relative populations of the (v'',J'') levels; the factors are valid for a particu-

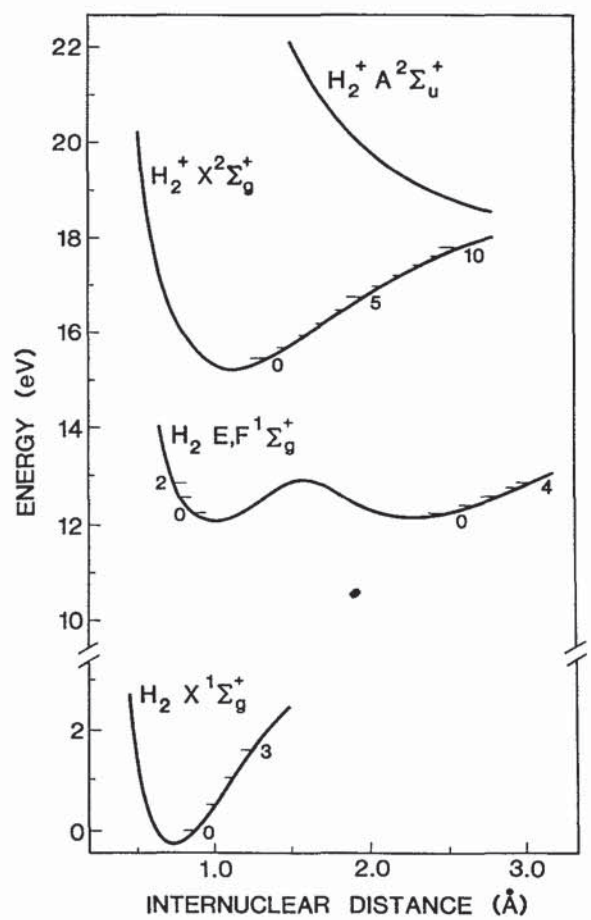

FIG. 1. Potential energy curves relevant to (2 + 1) REMPI of molecular hydrogen.

[a] Present address: AT&T Bell Laboratories, Room 1D354, 600 Mountain Avenue, Murray Hill, New Jersey 07974.

 0021-9606/91/130214-12$03.00

lar range of photon densities. The experimental correction factors are of two kinds: rotational correction factors, which are inversely proportional to rotational cross sections and are determined for each vibrational band independently, and vibrational correction factors, which are proportional to relative vibrational cross sections. Hence, the rotational correction factors multiply the ion signals to yield relative rotational populations, whereas the ion signals are divided by the vibrational correction factors to yield relative vibrational populations. The correction factors are determined for the following levels: H_2 ($v''=0, J''=0,2$–$4,6$–15), H_2 ($v''=1$, $J''=2$–$11,13$), H_2 ($v''=2$, $J''=2$–7); HD ($v''=0$, $J''=0$–13), HD ($v''=1, J''=2$–11), HD ($v''=2, J''=2$–8); and D_2 ($v''=0, J''=0$–17), D_2 ($v''=1, J''=3$–14), D_2 ($v''=2$, $J''=2$–11). The correction factors show a marked dependence on v'' but are nearly unity for all J'' values except H_2 ($v''=0, J''=12$–15). For these H_2 levels, the correction factors display a dramatic oscillation with J''.

The correction factors reported here do not rely on any theoretical description of the (2 + 1) REMPI process. Hence, they can be applied to extract relative population distributions from any experiment using (2 + 1) REMPI detection of molecular hydrogen under conditions similar to the present study. However, the experimentally determined correction factors can be compared with those derived from theoretical calculations of the H_2, HD, and D_2 $E, F\,^1\Sigma_g^+$ ($v'_E=0$, $J'=J''$)–$X\,^1\Sigma_g^+$ (v'',J'') two-photon transition moments (see Paper I[21]), provided that the ionization step has insignificant (v'',J'')-dependent structure. Previously, we have considered this comparison for some (v'',J'') levels of HD;[22] the present work extends the HD results and presents new results for H_2 and D_2. These comparisons provide a physical interpretation for the variation of the correction factors with v'' and J''. Moreover, they indicate the conditions under which the use of theoretical correction factors is justified when experimental values are unavailable.

II. EXPERIMENTAL

The experimental setup (Fig. 2) was identical to that previously described.[22–24] H_2, HD, or D_2 molecules were rotationally and vibrationally excited in a high-temperature tungsten oven (Fig. 3), which was mounted in the source chamber. Gas flowed effusively from the oven through an aperture into the ionization chamber, where it was intersected by a laser beam that caused (2 + 1) REMPI. Mass-selective ion detection was achieved by a shuttered time-of-flight mass spectrometer (TOF/MS),[24] which was located in the detection chamber. The vacuum chambers were differentially pumped to avoid the introduction of a large background of rotationally and vibrationally relaxed molecules into the ionization region and to minimize the pressure in the detection chamber.

The resistively heated oven consisted of two concentric, tungsten tubes (Ultramet) connected at their tips. The inner tungsten tube (2.75 mm i.d., 14 cm length, 0.25 mm wall thickness) contained the gas. A tungsten plate with an aperture between 25 and 75 μm in diameter (Ted Pella, Inc.) was electron beam welded to the tip of this tube. The outer tungsten tube (4.7 mm i.d., 0.76 mm wall thickness) was concentric to the inner tube. Current flowed from the outer to the inner tube, which had a smaller cross section. The current for the resistive heating was provided by a variable transformer (Variac) in combination with a step-down transformer. There was no permanent joint between the tubes. Instead, the tips of the two tubes were pressed together by a

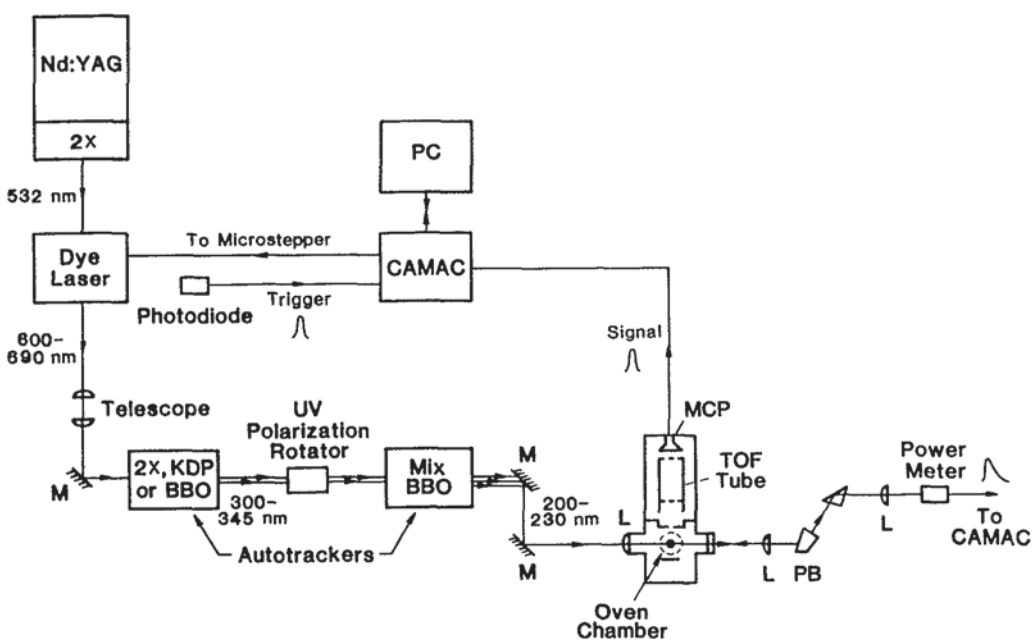

FIG. 2. Diagram of experimental setup.

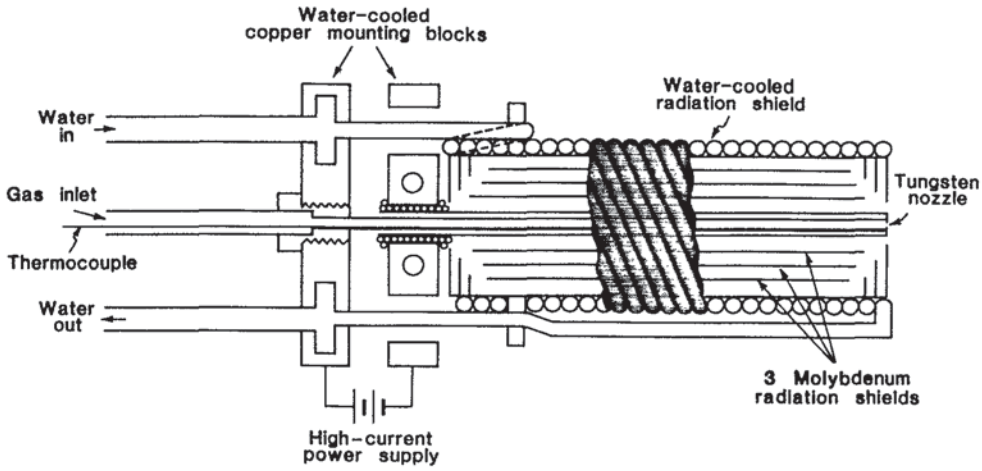

FIG. 3. Cross sectional view of the tungsten high-temperature oven.

spring-loaded mechanism. This design ensured good electrical contact, even at elevated temperatures. The inner tube was coated with ceramic cement (Aremco) to prohibit accidental electrical contact at any place other than the tip. Three molybdenum radiation shields isolated the outer tube from a water-cooled copper wall (5.1 cm o.d.). The oven was mounted on an adjustable bellows assembly to allow its positioning with respect to the laser beam.

The nozzle temperature was measured by two thermocouples located inside the inner tube close to the tip. The thermocouples were made of a W/5% Re and W/26% Re wire (Omega Engineering, Inc.); they are stable in hydrogen or an inert gas atmosphere up to 2750 K. The two pairs of thermocouple wires were insulated from each other and the oven walls by alumina (99.8% Al_2O_3) beads. The thermoelectric voltage was converted into a temperature reading by a calibrated indicator (Omega). For a given oven temperature, the indicator readings of the two thermocouples differed by less than 3 K.

The rovibrationally excited molecules entered the ionization chamber through a 2.5 mm diameter aperture. The distance from the oven to the aperture was approximately 1 cm. The laser beam ($\lambda \sim 215$ nm) intersected the gas beam approximately 6 cm downstream from the nozzle tip for (2 + 1) REMPI detection of the hydrogen molecules. The ~ 215 nm radiation was generated by a pulsed (10 Hz) Nd:YAG-pumped dye laser (DCR-3G, PDL-1, Spectra-Physics; R640/DCM dye, Exciton) with frequency-doubling and mixing stages (Autotracker II, Inrad). The dye-laser light (603–687 nm) was frequency doubled in β-barium borate (BBO, 40° cut).[25] The residual dye-laser light was mixed with the doubled light in a second BBO crystal (70° cut) to yield 1.0–3.0 mJ per pulse of horizontally polarized radiation at 201–229 nm. The probe beam was focused (Esco, Suprasil B, $f = 125$ mm) to a spot size of approximately 100 μm to give a power density of approximately 4 GW/cm^2 in a 5 ns pulse.

The ions were formed between two charged, parallel plates that accelerated them into the detection chamber that contained the shuttered TOF/MS.[24] The laser power and the time-gated ion current at the CEMA detector were recorded for each laser shot as a function of laser frequency by a computer-interfaced CAMAC system.[26] Each spectral peak was corrected for laser power variations (Sec. III B) and integrated to obtain the ion signal associated with the population in the given quantum state.

(2 + 1) REMPI spectra of H_2, HD, and D_2 were recorded for two-photon Q-branch transitions connecting (v'',J'') levels of the $X\,^1\Sigma_g^+$ ground state to $(v'_E = 0, J' = J'')$ levels of the $E, F\,^1\Sigma_g^+$ excited electronic state, which are subsequently photoionized to yield $X\,^2\Sigma_g^+$ (v^+,J^+) levels of the molecular ion. Ion signals were measured for the following levels: H_2 $(v'' = 0, J'' = 0,2\text{–}4,6\text{–}15)$, $(v'' = 1, J'' = 2\text{–}11,13)$, $(v'' = 2, J'' = 2\text{–}7)$; HD $(v'' = 0, J'' = 0\text{–}13)$, $(v'' = 1, J'' = 2\text{–}11)$, $(v'' = 2, J'' = 2\text{–}8)$; and D_2 $(v'' = 0, J'' = 0\text{–}17)$, $(v'' = 1, J'' = 3\text{–}14)$, $(v'' = 2, J'' = 2\text{–}11)$.

Oven measurements were performed with temperatures from 480–1820 K, pressures from 26–214 Torr, and orifice diameters from 25–75 μm. The oven was not used for room-temperature measurements of the lowest $v'' = 0$ rotational levels. Instead, a mixture of 2%–5% H_2, HD, or D_2 in Ar was bled into the ionization chamber, where the pressure was maintained at $\sim 2 \times 10^{-6}$ Torr. Higher partial pressures of hydrogen resulted in space-charge broadening of the TOF peaks and nonlinear detector response.

III. RESULTS

A. Calibration standard

We use the internal state distribution of the hydrogen issuing from the oven to calibrate the (2 + 1) REMPI-TOF/MS detection procedure, which requires that this distribution be known. Therefore, the oven was operated in a regime for which the rovibrational population distribution of the hydrogen beam was Boltzmann. Two experimental conditions had to be fulfilled: (a) the stagnation time of hydrogen molecules in the heated nozzle had to be long enough

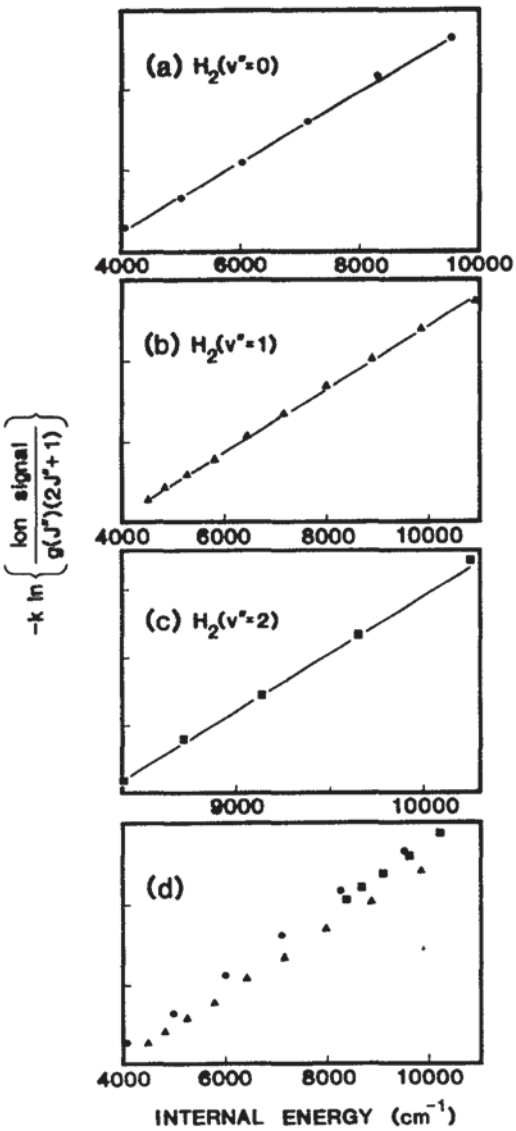

FIG. 4. Boltzmann plots for (a) H_2 ($v''=0$), (b) H_2 ($v''=1$), and (c) H_2 ($v''=2$). The three vibrational bands are plotted on the same energy scale in (d). These plots are based on data taken with the oven source. Error bars (one standard deviation) are the same size as or smaller than the symbols.

to ensure the molecules equilibrated to a temperature; and (b) the molecules could not undergo relaxation upon issuing from the oven. These conditions have been shown[22] to be fulfilled for HD, which has the highest energy-transfer rates of the three hydrogen isotopomers.[18,27–30] We provide verification here that both criteria were also satisfied for H_2 and D_2.

The dwell time of the molecules in the heated nozzle is calculated to be 0.5–1.3 s, in which time each molecule undergoes at least 10^8 hard-sphere collisions (0.27 nm^2 cross section).[31] Vibration-to-translation (V–T) transfer rates for H_2 have been measured[32–36] and calculated.[37] At 1500 K, approximately 7×10^5 collisions are required to transfer H_2 ($v''=0$) to H_2 ($v''=1$).[32,37] Consequently, each H_2 molecule experiences more than 100 v''-changing collisions within the nozzle. The room-temperature V–T rate for H_2 ($v''=2$) is approximately ten times faster than for H_2 ($v''=1$).[36] Assuming the H_2 ($v''=2$) V–T rate at 1500 K is at least as large as the H_2 ($v''=1$) V–T rate at that temperature, the stagnation time is sufficient to ensure complete vibrational equilibrium of the H_2 to the nozzle temperature. In addition, V–V energy transfer $[H_2(v''=0)+H_2(v''=2)\rightarrow 2H_2(v''=1)]$ contributes to the attainment of vibrational equilibrium.[36,38] The vibrational equilibration of H_2 is the slowest energy-transfer process; D_2[30,39–41] and HD[27] require fewer collisions than H_2 for V–T transfer. Furthermore, rotational energy transfer rates[18] are several orders of magnitude faster than those for V–T transfer, ensuring that thermal equilibrium [criterion (a)] is attained for all three gases. Criterion (b) has been shown[22] to be satisfied for HD under the present experimental conditions. Since HD has the highest rotational relaxation rate[18] of the three isotopomers, criterion (b) is expected to hold for H_2 and D_2 as well.

We analyzed the data by plotting the natural logarithm of the ion signal divided by the rotational degeneracy, $(2J''+1)$, and the nuclear spin degeneracy $g(J'')$ vs the internal energy to produce what is called a Boltzmann plot. To generate each Boltzmann plot, power-corrected, integrated ion signals from three scans of a given rotational distribution were individually normalized and then averaged. Representative Boltzmann plots for H_2 are given in Fig. 4; Boltzmann plots for HD and D_2 are similar. For each data set, a weighted linear least-squares fit of the points in the Boltzmann plot was performed. The slope of the fitted line is inversely proportional to the gas temperature. The ground-state energies were calculated using the spectroscopic constants given by Huber and Herzberg.[42] Excluding the lowest J'' levels for $v''=1$ and 2, all data points within each vibrational level fall on a straight line. The low rotational levels were contaminated by background gas that was relaxed rotationally but not vibrationally. This background contribution could be reduced, though not eliminated, by placing a smaller aperture between the source chamber and the ionization chamber, but this alteration would be made at the expense of signal intensity. Consequently, we excluded the following levels from further analysis: all molecules ($v''=1$ and 2, $J''=0$ and 1) and D_2 ($v''=1, J''=2$).

In the oven scans, the temperatures derived from the Boltzmann fits differed from the thermocouple readings. For all three vibrational levels of all gases, the temperature was $11.6\% \pm 1.5\%$ lower than the thermocouple reading. This deviation was not correlated to either pressure or thermocouple reading, further demonstrating that the molecules did not relax upon exiting the oven. The slope of the Boltzmann plot of the room-temperature background hydrogen corresponds to 289 ± 11 K (average of H_2, HD, and D_2 results), in good agreement with the room temperature of $\sim$293 K.

B. Power dependence

In these measurements, the dye laser was scanned over 84 nm. Dye mixes were developed that have relatively flat gain over this spectral region,[43] but power variations could not be completely eliminated. To determine how the ion sig-

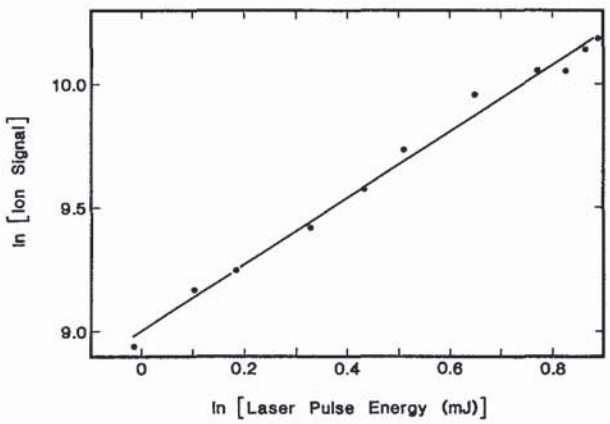

FIG. 5. Plot of ion signal vs laser power for the (2 + 1) REMPI process for H_2 ($v'' = 1, J'' = 5$). The solid line represents a linear least-squares fit to the data points.

TABLE I. H^+/H_2^+ ratio in (2 + 1) REMPI via the $E,F\,^1\Sigma_g^+$ ($v'_E = 0, J' = J''$)–$X\,^1\Sigma_g^+$ (v'', J'') transition.

J''	$[H^+/H_2^+]$[a] $v'' = 0$	$v'' = 1$
1	···	0.050 ± 0.008
2	0.13 ± 0.01	···
3	···	0.047 ± 0.014
4	0.15 ± 0.03	···
5	···	0.059 ± 0.003
6	0.15 ± 0.01	···
7	0.17 ± 0.03	0.084 ± 0.006
8	0.18 ± 0.04	···
9	0.20 ± 0.05	···
10	0.30 ± 0.01	···
11	0.32 ± 0.05	···
12	0.50 ± 0.14	···

[a] Uncertainties represent one standard deviation.

nal varied with laser power, several rotational levels of H_2 ($v'' = 0,1$) were measured as a function of laser pulse energy. The laser power was varied by up to a factor of 2.5. Results of this study for H_2 ($v'' = 1, J'' = 5$) are shown in Fig. 5. The slope of the line in this figure gives the laser power dependence of the ion signal. The ion signal was found to be proportional to the laser pulse energy raised to the 1.4 ± 0.2 power, indicating that saturation had occurred; in the absence of saturation the power dependence would be quadratic or higher. In a separate experiment, saturation of the ionization step was confirmed for several rotational levels of HD ($v'' = 0,1$) by using a second, time-delayed laser pulse ($\lambda = 266$ nm) to ionize the metastable HD that had not been ionized by the ~215 nm pulse.[44] For the highly populated, low-J'' levels, 97% ± 3% of the excited molecules were ionized by the detection laser. For less populated levels, saturation could not be quantified but was confirmed qualitatively. Hence, any laser power dependence arising from the ionization step was eliminated. The 1.4 ± 0.2 power dependence indicates that saturation had also occurred in the two-photon step.

We assumed that the HD and D_2 ion signals had the same probe-laser power dependence as that of H_2. This assumption is reasonable because both the laser pulse energies employed and the two-photon cross sections[21] are comparable for all three gases. Analysis of the data incorporated this laser pulse energy dependence of the ion signal.

C. Proton production

Proton production competes with direct ionization in the (2 + 1) REMPI process. Because we detect only the molecular ion, the production of protons following the resonant two-photon excitation into the E, F state must be considered. To evaluate the significance of loss mechanisms associated with proton production, the H^+/H_2^+ ratio was determined experimentally. For this measurement, the apparatus was modified in one respect. Since the slit in the extractor plate could cause a discrimination against fast H^+ ions moving perpendicular to the detector axis, it was replaced by a grid. The H^+/H_2^+ ratio was determined for H_2 ($v'' = 0, J'' = 2,4,6$–12) and H_2 ($v'' = 1, J'' = 1,3,5,7$). Three scans of the H^+ and H_2^+ ion signals were recorded alternately. The integrated ion signals of these scans were averaged for each ionic species, and their ratio was taken. Between 5 and 15 ratios for each rotational level were measured on different days and under various experimental conditions. The results (see Table I and Fig. 6) can be summarized as follows:

(1) The H^+/H_2^+ ratio is approximately constant for H_2 ($v'' = 0, J'' = 2$–9) and H_2 ($v'' = 1, J'' = 1$–5).

(2) The H^+/H_2^+ ratio increases significantly between $J'' = 10$ and $J'' = 12$ for H_2 ($v'' = 0$).

(3) The H^+/H_2^+ ratio is approximately three times larger for H_2 ($v'' = 0$) than for H_2 ($v'' = 1$).

We also measured the probe-laser energy dependence of H^+ production. For H_2 ($v'' = 0, J'' = 8$) the H^+ signal was proportional to the laser pulse energy raised to the 2.1 pow-

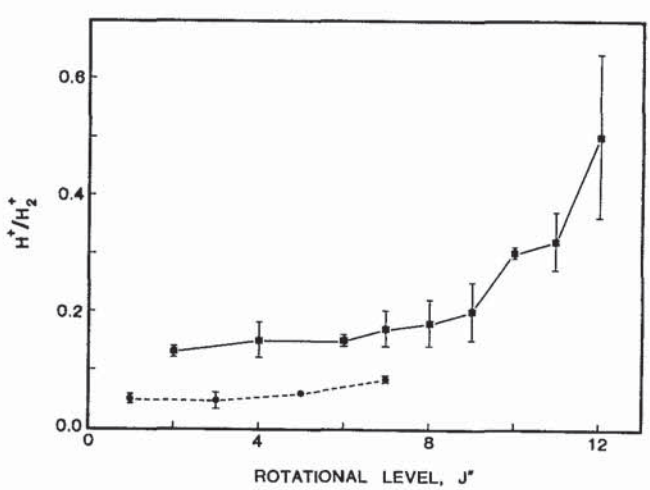

FIG. 6. Plot of the H^+/H_2^+ ratio as a function of the rotational quantum number J'' for H_2 ($v'' = 0$) (shown as squares) and H_2 ($v'' = 1$) (shown as circles).

er. Note that two different channels can lead to H^+ production. The first is direct excitation to the dissociative continuum of an H_2^+ state. Some of the H atom produced in the fragmentation might be ionized subsequently by the probe laser. For this channel, the measured H^+/H_2^+ represents an upper bound for the degree of fragmentation in the $(2+1)$ REMPI process. The second channel is excitation to a repulsive H_2 curve and subsequent ionization of the H atom by the probe laser. In this case, the H^+/H_2^+ ratio may represent a lower bound to the degree of fragmentation.

In an earlier study, Normand, Cornaggia, and Morellec[45] investigated the six-photon ionization of room-temperature H_2 in which four photons caused the resonant excitation into $v'_E = 0$. At a probe laser intensity (0.1–1.0 GW/cm^2) comparable to that used in our study, these workers observed significant H^+ production. The H^+/H_2^+ ratio was determined to be 0.2 for the $Q(1)$ line. This result is in good agreement with our measurements in which we found the H^+/H_2^+ ratio to be ~ 0.15 for the $J'' = 2$–6 range. Although the total excitation energy was the same in both studies, the number of photons causing ionization was different.

Buck, Parker, and Chandler[46] measured proton production in $(2+1)$ REMPI of room-temperature H_2 ($v'' = 0, J'' = 0$–3) at laser pulse energies approximately 40 times lower than those in this study. The H^+/H_2^+ ratio was found to be significant for ionization from excited (mainly odd) vibrational levels of the E, F state but insignificant for ionization following excitation into $v'_E = 0$. More recently, Buntine, Baldwin, and Chandler[47] remeasured the H^+/H_2^+ ratio for H_2 ($v'' = 0, J'' = 1$) at probe laser intensities comparable to the present study and found H^+ production of the same magnitude as reported here for low J'' levels of $v'' = 0$.

D. Calculation of correction factors

1. Experimental correction factors

We calculate rotational correction factors $C_J(J'')$ and then vibrational correction factors $C_v(v'')$. In this analysis, the gas temperature is assumed to be 11.6% less than the thermocouple reading, as indicated in the Boltzmann plots of all vibrational levels of H_2, HD, and D_2 (Sec. III A).

a. Rotational correction factors. Rotational correction factors are determined for each vibrational band. The intercept of a line of fixed slope (determined by the gas temperature) is adjusted to minimize the deviations $D(J'')$ of the data points from the line in a Boltzmann plot. These deviations are related to the rotational correction factors $C_J(J'')$ by

$$C_J(J'') = \exp[D(J'')/k], \tag{1}$$

where k is the Boltzmann constant. This procedure, which is based on relative ion signals, determines relative correction factors that are proportional to the inverse of the rotational cross sections. Hence, the measured ion signals must be *multiplied* by $C_J(J'')$ to obtain quantum-state populations. The rotational correction factors are given in Tables II–X and displayed in Figs. 7–9.

TABLE II. Rotational correction factors $C_J(J'')$ for the transition H_2 $E,F\,^1\Sigma_g^+$ ($v'_E = 0, J' = J''$)–$X\,^1\Sigma_g^+$ ($v'' = 0, J''$).

J''	Experimental[a]	Theoretical[b]
0	1.12 ± 0.09	1.034
1	···	1.031
2	1.04 ± 0.07	1.026
3	0.90 ± 0.06	1.019
4	0.88 ± 0.06	1.010
5	···	0.999
6	1.03 ± 0.04	0.987
7	0.94 ± 0.04	0.975
8	0.99 ± 0.11	0.958
9	0.90 ± 0.12	0.942
10	0.95 ± 0.12	0.927
11	1.04 ± 0.11	0.911
12	1.62 ± 0.32	0.977
13	1.44 ± 0.27	0.867
14	2.61 ± 0.67	1.076
15	1.72 ± 0.36	0.812

[a] Uncertainties represent one standard deviation.
[b] From Ref. 21.

TABLE III. Rotational correction factors $C_J(J'')$ for the transition H_2 $E,F\,^1\Sigma_g^+$ ($v'_E = 0, J' = J''$)–$X\,^1\Sigma_g^+$ ($v'' = 1, J''$).

J''	Experimental[a]	Theoretical[b]
0	···	1.085
1	···	1.080
2	0.94 ± 0.10	1.075
3	1.04 ± 0.04	1.066
4	0.99 ± 0.03	1.055
5	0.99 ± 0.05	1.041
6	0.99 ± 0.05	1.025
7	0.99 ± 0.06	1.009
8	1.05 ± 0.07	0.987
9	1.00 ± 0.06	0.966
10	1.03 ± 0.16	0.945
11	1.07 ± 0.23	0.921
12	···	0.959
13	1.14 ± 0.29	0.870
14	···	1.085
15	···	0.806

[a] Uncertainties represent one standard deviation.
[b] From Ref. 21.

TABLE IV. Rotational correction factors $C_J(J'')$ for the transition H_2 $E,F\,^1\Sigma_g^+$ ($v'_E = 0, J' = J''$)–$X\,^1\Sigma_g^+$ ($v'' = 2, J''$).

J''	Experimental[a]	Theoretical[b]
0	···	1.057
1	···	1.051
2	1.04 ± 0.12	1.045
3	0.98 ± 0.08	1.036
4	1.01 ± 0.07	1.023
5	1.00 ± 0.07	1.008
6	1.08 ± 0.17	0.989
7	0.96 ± 0.16	0.971
8	···	0.946
9	···	0.921
10	···	0.897
11	···	0.869
12	···	0.913
13	···	0.813
14	···	1.000
15	···	0.750

[a] Uncertainties represent one standard deviation.
[b] From Ref. 21.

TABLE V. Rotational correction factors $C_J(J'')$ for the transition HD $E,F\,^1\Sigma_g^+\,(v'_E=0,J'=J'')$–$X\,^1\Sigma_g^+\,(v''=0,J'')$.

J''	Experimental[a]	Theoretical[b]
0	0.96 ± 0.03	1.065
1	0.99 ± 0.02	1.062
2	1.05 ± 0.05	1.059
3	0.97 ± 0.03	1.054
4	0.95 ± 0.05	1.047
5	0.93 ± 0.10	1.039
6	0.99 ± 0.08	1.029
7	1.01 ± 0.03	1.018
8	0.98 ± 0.02	1.006
9	0.96 ± 0.03	0.994
10	1.04 ± 0.07	0.981
11	1.11 ± 0.06	0.968
12	1.09 ± 0.09	0.955
13	1.18 ± 0.14	0.934

[a] Uncertainties represent one standard deviation.
[b] From Ref. 21.

Figures 7–9 show that the rotational correction factors are essentially unity except for high J'' levels. Thus for low to intermediate J'' levels no correction is needed to convert ion signals to relative quantum-state populations under the present experimental conditions.

b. Vibrational correction factors. Relative vibrational correction factors are determined by adopting the arbitrary standard that the correction factor for $v''=0$ is unity, i.e., $C_v(0)\equiv 1.0$. The following analysis yields the ratio of the correction factors between two adjacent vibrational levels v''_a and v''_b. Ion signals of rotational levels in two adjacent vibrational bands were recorded sequentially under identical experimental conditions. When the rotational distributions are graphed on the same Boltzmann plot, the vibrational bands are displaced from each other [see Fig. 4(d)]. The ratio $C_v(v''_a)/C_v(v''_b)$ is related to the two intercepts $I(v''_a)$ and $I(v''_b)$ by

TABLE VI. Rotational correction factors $C_J(J'')$ for the transition HD $E,F\,^1\Sigma_g^+\,(v'_E=0,J'=J'')$–$X\,^1\Sigma_g^+\,(v''=1,J'')$.

J''	Experimental[a]	Theoretical[b]
0	···	1.063
1	···	1.059
2	0.99 ± 0.07	1.055
3	1.03 ± 0.04	1.049
4	0.95 ± 0.04	1.041
5	0.99 ± 0.08	1.031
6	0.99 ± 0.06	1.019
7	0.99 ± 0.08	1.006
8	0.98 ± 0.05	0.992
9	1.03 ± 0.08	0.976
10	1.05 ± 0.13	0.959
11	1.07 ± 0.16	0.942
12	···	0.924
13	···	0.903
14	···	0.886

[a] Uncertainties represent one standard deviation.
[b] From Ref. 21.

TABLE VII. Rotational correction factors $C_J(J'')$ for the transition HD $E,F\,^1\Sigma_g^+\,(v'_E=0,J'=J'')$–$X\,^1\Sigma_g^+\,(v''=2,J'')$.

J''	Experimental[a]	Theoretical[b]
0	···	1.030
1	···	1.025
2	1.06 ± 0.07	1.021
3	1.05 ± 0.05	1.015
4	1.02 ± 0.04	1.005
5	0.98 ± 0.04	0.994
6	0.97 ± 0.05	0.981
7	0.92 ± 0.06	0.966
8	0.93 ± 0.13	0.949
9	···	0.931
10	···	0.911
11	···	0.891
12	···	0.869
13	···	0.850
14	···	0.824

[a] Uncertainties represent one standard deviation.
[b] From Ref. 21.

$$C_v(v''_a)/C_v(v''_b)=\exp\{[I(v''_a)-I(v''_b)]/k\}. \qquad (2)$$

These intercepts are determined from least-squares fits of straight lines of fixed slope (temperature) to the data points in each vibrational band; any highly deviant levels are omitted. The vibrational correction factors determined in this analysis correspond to relative vibrational cross sections. Hence, the ion signals must be *divided* by $C_v(v'')$ to compare populations in different vibrational bands.

Table XI shows that the vibrational correction factors differ substantially from unity. In particular, $(2+1)$ REMPI is more sensitive to $v''=1$ and $v''=2$ than to $v''=0$ for H_2, HD, and D_2.

2. Theoretical correction factors

The calculation of the theoretical correction factors is based on the two-photon cross sections $|M_{fo}|^2$ for the E–X

TABLE VIII. Rotational correction factors $C_J(J'')$ for the transition D_2 $E,F\,^1\Sigma_g^+\,(v'_E=0,J'=J'')$–$X\,^1\Sigma_g^+\,(v''=0,J'')$.

J''	Experimental[a]	Theoretical[b]
0	1.04 ± 0.06	1.091
1	1.02 ± 0.03	1.089
2	0.94 ± 0.03	1.087
3	1.04 ± 0.04	1.083
4	1.01 ± 0.05	1.079
5	0.97 ± 0.07	1.074
6	0.97 ± 0.09	1.068
7	1.06 ± 0.05	1.060
8	1.17 ± 0.11	1.053
9	1.04 ± 0.06	1.045
10	1.07 ± 0.10	1.036
11	1.00 ± 0.04	1.026
12	0.92 ± 0.05	1.017
13	0.90 ± 0.05	1.008
14	0.90 ± 0.04	0.998
15	1.05 ± 0.10	0.989
16	1.23 ± 0.18	0.973
17	1.42 ± 0.41	0.975

[a] Uncertainties represent one standard deviation.
[b] From Ref. 21.

TABLE IX. Rotational correction factors $C_J(J'')$ for the transition D_2 $E,F\,^1\Sigma_g^+$ $(v'_E=0, J'=J'')$–$X\,^1\Sigma_g^+$ $(v''=1, J'')$.

J''	Experimental[a]	Theoretical[b]
0	···	1.021
1	···	1.019
2	···	1.017
3	1.04 ± 0.10	1.013
4	1.04 ± 0.10	1.008
5	1.05 ± 0.07	1.002
6	0.96 ± 0.08	0.995
7	1.00 ± 0.05	0.986
8	0.96 ± 0.06	0.977
9	0.97 ± 0.06	0.967
10	0.89 ± 0.08	0.956
11	0.90 ± 0.10	0.945
12	0.90 ± 0.11	0.933
13	0.98 ± 0.16	0.921
14	0.92 ± 0.17	0.908
15	···	0.896
16	···	0.880
17	···	0.871

[a] Uncertainties represent one standard deviation.
[b] From Ref. 21.

transition (see Paper I[21]). Note that theory predicts absolute cross sections, whereas experiment measures only relative cross sections. Hence, we must derive relative theoretical cross sections that can be compared to experiment.

The experimental correction factors $C_J(J'')$ are proportional to the inverse of the rotational cross sections. Therefore, we take the sums of the reciprocals of the theoretical two-photon transition moments $|M_{fo}|^2$ and rescale so that this sum equals the sum of the ion signals for the J'' levels in common with the experimental distribution.

The calculation of vibrational correction factors from the reported two-photon transition moments is more in-

TABLE X. Rotational correction factors $C_J(J'')$ for the transition D_2 $E,F\,^1\Sigma_g^+$ $(v'_E=0, J'=J'')$–$X\,^1\Sigma_g^+$ $(v''=2, J'')$.

J''	Experimental[a]	Theoretical[b]
0	···	1.030
1	···	1.027
2	1.00 ± 0.05	1.024
3	1.09 ± 0.03	1.019
4	0.97 ± 0.05	1.013
5	1.04 ± 0.04	1.006
6	1.05 ± 0.05	0.998
7	0.99 ± 0.07	0.988
8	0.89 ± 0.04	0.977
9	0.97 ± 0.10	0.965
10	0.96 ± 0.08	0.952
11	0.92 ± 0.15	0.938
12	···	0.923
13	···	0.908
14	···	0.891
15	···	0.876
16	···	0.859
17	···	0.840

[a] Uncertainties represent one standard deviation.
[b] From Ref. 21.

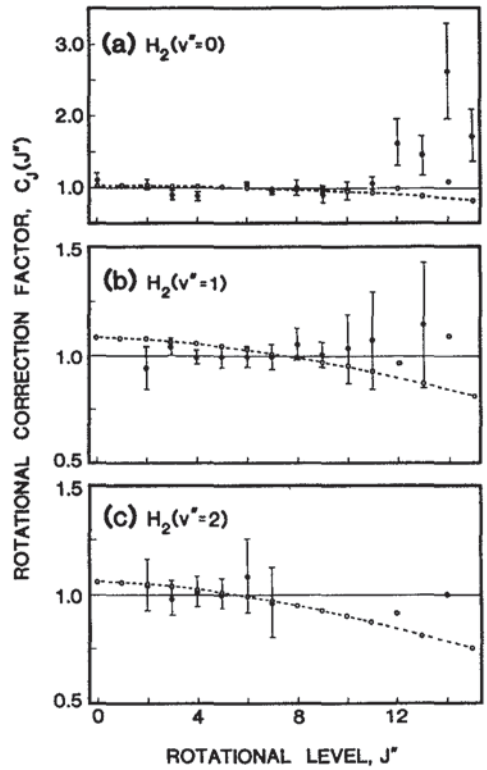

FIG. 7. Experimental (solid) and theoretical (open) rotational correction factors $C_J(J'')$ as a function of the rotational quantum number J'' for (a) H_2 $(v''=0)$, (b) H_2 $(v''=1)$, and (c) H_2 $(v''=2)$. Error bars represent one standard deviation. The theoretical values are connected by a dashed line to guide the eye.

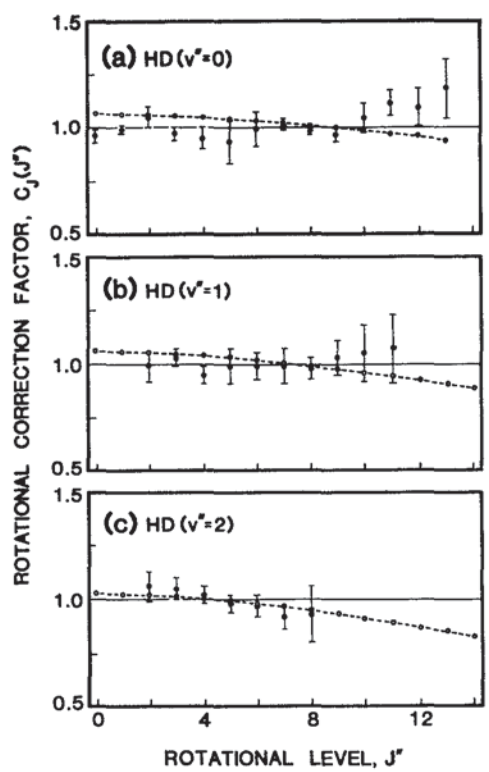

FIG. 8. Experimental (solid) and theoretical (open) rotational correction factors $C_J(J'')$ as a function of the rotational quantum number J'' for (a) HD $(v''=0)$, (b) HD $(v''=1)$, and (c) HD $(v''=2)$. Error bars represent one standard deviation. The theoretical values are connected by a dashed line to guide the eye.

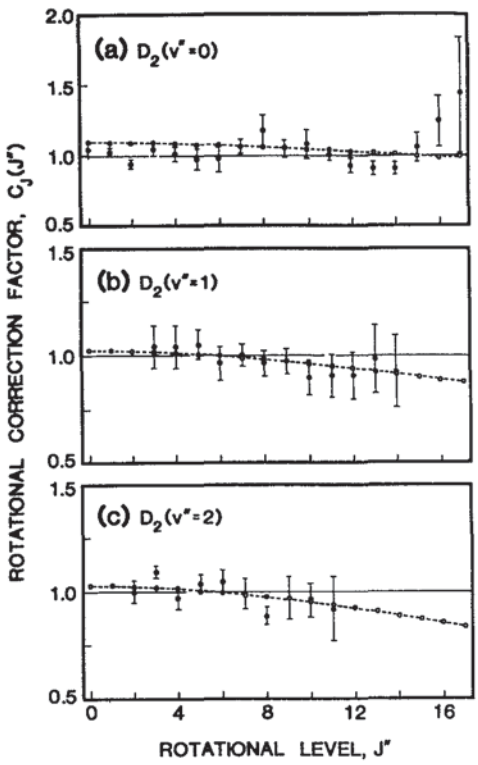

FIG. 9. Experimental (solid) and theoretical (open) rotational correction factors $C_J(J'')$ as a function of the rotational quantum number J'' for (a) D_2 ($v''=0$), (b) D_2 ($v''=1$), and (c) D_2 ($v''=2$). Error bars represent one standard deviation. The theoretical values are connected by a dashed line to guide the eye.

volved. The experimental vibrational correction factors $C_v(v'')$ are calculated from Eq. (2). This equation uses the intercepts determined from least-squares fits of straight lines to the data points in each vibrational band; hence, the resulting vibrational correction factors represent J''-averaged relative vibrational cross sections. The average extends over the particular range of J'' recorded for a specific vibrational band. The derivation of equivalent theoretical values for a direct comparison requires an average $|M_{fo}|^2$ value for the experimentally observed J'' range. These average values of $|M_{fo}|^2$ are then rescaled such that, as in the experimental case, $C_v(v'')=1$. This procedure is justified so long as the dependence on v'' is larger than on J''. Consequently, strongly deviant levels, such as H_2 ($v=0, J=12,14$), are omitted in the derivation of the experimental and theoretical vibrational correction factors.

TABLE XI. Vibrational correction factors $C_v(v'')$ for the (2 + 1) REMPI detection of molecular hydrogen via the transition $E,F\,^1\Sigma_g^+\,(v'_E=0,J'=J'')$–$X\,^1\Sigma_g^+\,(v''_J,J'')$.

Molecule	v''	Experimental[a]	Theoretical[b]
	0	1.0	1.0
H_2	1	2.6 ± 0.5	3.0 ± 0.3
	2	2.3 ± 0.5	3.2 ± 0.2
	0	1.0	1.0
HD	1	2.7 ± 0.3	3.2 ± 0.2
	2	3.2 ± 0.9	4.1 ± 0.2
	0	1.0	1.0
D_2	1	3.0 ± 0.8	3.8 ± 0.2
	2	3.9 ± 1.6	5.9 ± 0.3

[a] Uncertainties represent one standard deviation.
[b] From Ref. 21. Uncertainties represent one standard deviation of the average over J'' of $C_v(v'')$.

IV. DISCUSSION

We have quantitatively determined the relationship between ion signals and quantum-state populations in the (2 + 1) REMPI detection of H_2 ($v''=0,1,2$), HD ($v''=0,1,2$), and D_2 ($v''=0,1,2$). The experimentally determined correction factors, based on calibration against a thermal effusive beam, are independent of any theoretical description of the multiphoton ionization process. In the following discussion, we first compare the experimental correction factors with those derived from the theoretical treatment of the two-photon step in the (2 + 1) REMPI process (Paper I[21]). Then we discuss possible reasons for deviations from the theoretical predictions and indicate the conditions under which theory can be trusted to provide a realistic estimate of the correction factors in the absence of experimental measurements.

For an ideal comparison of experimental and theoretical correction factors, the ion signal must have no dependence on the ionization step of the (2 + 1) REMPI process and the bound–bound step should remain unsaturated. In our experimental configuration we saturated the ionization step (Sec. III B), which eliminated laser intensity dependence. However, the possibility remains of a wavelength dependence of the yield of the molecular ion; this dependence is caused by dissociation into neutral or ionic fragments. In addition, the two-photon step in our experiment was saturated (Sec. III B). Although our data analysis incorporated the correct power dependence, the saturation still may introduce discrepancies between experiment and theory.

A. Rotational correction factors

For almost all of the measured rovibrational levels, the experimental and theoretical correction factors agree within experimental uncertainty (see Figs. 7–9). In general, theory predicts slow decreases in $C_J(J'')$ with increasing J'' for all v'' and all gases.[21] This prediction corresponds to slow increases in the two-photon transition moments with J''. However, this trend is so weak that it is difficult to assess whether the experimental data are better described as following it or scattering about unity. Moreover, because there is saturation of the two-photon step (Sec. III B), any dependence on J'' is flattened.

Marked deviations occur between theory and experiment for $v''=0$ and high J'', particularly for H_2 ($v''=0$, $J''=12$–15). Although theory also predicts fluctuations in $C_J(J'')$ for these levels, caused by tunneling in the double well of the E,F state,[21] these fluctuations are much smaller than those observed experimentally.

Because we detect only the molecular ion, possible effects of (blind) dissociation channels that produce H^+ and

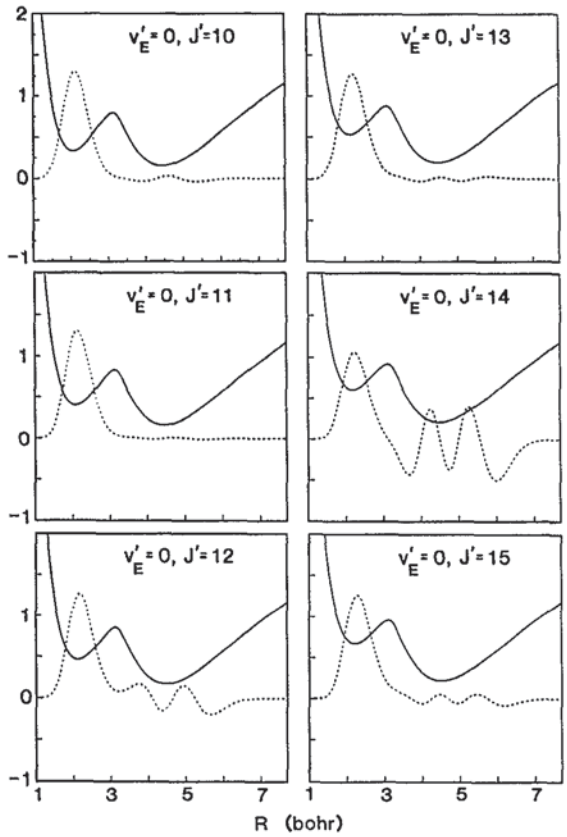

FIG. 10. H_2 $E, F\,^1\Sigma_g^+$ potential energy curves (solid lines) for $J' = 10$–15 and corresponding $v'_E = 0$ vibrational wave functions (dashed lines).

H must be addressed. Both a direct dissociative ionization process and a dissociative process with subsequent ionization can produce H^+.[45,46,48–58] At the photon energies used in this experiment, (2 + 1) REMPI can access the dissociative continua of the $X\,^2\Sigma_g^+$ state of H_2^+ or the repulsive $A\,^2\Sigma_u^+$ state. Note that excitation to $A\,^2\Sigma_u^+$ from the $v'_E = 0$ level is a two-electron transition but it is a one-electron transition from a v'_F level. Thus, dissociative ionization through the $A\,^2\Sigma_u^+$ state is negligible except when tunneling from the $v'_E = 0$ to v'_F level is important, e.g., at $J'' = 12$ for H_2. (See Fig. 10 for a plot of the vibrational wave functions of the $v'_E = 0$ level for $J' = 10$–15.) Dissociative ionization through the H_2^+ $A\,^2\Sigma_u^+$ state explains neither the observed H^+/H_2^+ ratio of 0.15 for $J'' = 2$–6 at $v'' = 0$ nor the gradual increase to 0.32 at $J'' = 11$. On the other hand, excitation to the dissociative continuum of the H_2^+ $X\,^2\Sigma_g^+$ state is a dipole-allowed process. A study[59] of the Franck–Condon factors between the $v'_E = 0$ level and the accessible range of the $X\,^2\Sigma_g^+$ continuum indicates that they slowly increase with J'' at low J''. This trend is partly caused by an increase of the accessible continuum with J''. In addition, tunneling into the F well increases the overlap with the H_2^+ $X\,^2\Sigma_g^+$ continuum; this may account for the fluctuations in the experimental $C_J(J'')$ at high J''.

Another possible source of H or H^+ is excitation to a predissociative state of H_2. The potential energy curves of the Rydberg states that converge to excited states of H_2^+ cross curves of doubly excited states, leading to dissociation.[60–62] This mechanism may compete with direct molecular ionization and could cause fluctuations in $C_J(J'')$. However, we observed no fluctuations in $C_J(J'')$ for low J'' and a constant H^+/H_2^+ ratio ($\sim$0.15). The absence of fluctuations is a fortuitous consequence of the fact that the total energy region accessed in the REMPI detection scheme lies between two Rydberg series.

Finally, we point out that the E state acquires a predissociative width caused by nonadiabatic coupling with the dissociative continuum of the X state.[63] For $v'_E = 0$ and low J', this width is negligibly small, although its dependence on J' has not been established.

B. Vibrational correction factors

We determine an average $C_v(v'')$ because the dependence of the ion signal on v'' is generally stronger than on J''. Similarly, the theoretical $C_v(v'')$ values represent averages over J'' for the range of J'' levels studied experimentally (again omitting any deviant levels). The experimental and theoretical results (Table XI) are in good agreement within the combined uncertainties. Here we seek an explanation for the trends in the vibrational correction factors, namely, (2 + 1) REMPI is two to three times more sensitive to $v'' = 1$ and $v'' = 2$ than to $v'' = 0$ and the experimental correction factors are systematically smaller than the theoretical ones. The dependence of the two-photon transition moment on v'' accounts for the first trend. We suggest that two different mechanisms contribute to the second trend: the change in the H^+/H_2^+ ratio with wavelength (i.e., v'') and the effect of saturation on the two-photon transitions.

Recall that the theoretical calculations do not include the ionization step. The measurements (Table I and Fig. 6) of the H^+/H_2^+ ratio from H_2 ($v'' = 0,1$) demonstrate that one or more dissociative processes compete with direct ionization. The H^+/H_2^+ ratio is smaller for $v'' = 1$ than $v'' = 0$. We speculate that this behavior reflects in part the wavelength dependence of H^+ production via transitions to the continuum of the H_2^+ $X\,^2\Sigma_g^+$ state. The variation of the H^+/H_2^+ ratio with v'' is in the opposite direction to the disagreement between theory and experiment for the variation of $C_v(v'')$ with v''. In other words, taking H^+ production into account increases this discrepancy.

Saturation of the two-photon step in the (2 + 1) REMPI process causes weaker transitions to be detected with a greater sensitivity than in the absence of saturation. Recall that the power dependence of the molecular ion signal was 1.4 ± 0.2, which is interpreted as evidence for saturation of the two-photon transition (since the ionization step was determined independently to be saturated). Moreover, a simple estimate indicates that we operated under saturation conditions for the two-photon transition.[22,64] Because the two-photon transition moments from $v'' = 1$ and $v'' = 2$ are similar, their degree of saturation is comparable. We note that the agreement between the theoretical and experimental $C_v(v'' = 1)/C_v(v'' = 2)$ ratios is better than that between the ratios $C_v(v'' = 1 \text{ or } 2)/C_v(v'' = 0)$. This observation supports the conjecture that saturation contributes to the discrepancy between theory and experiment for $C_v(v'')$.

V. SUMMARY

We have calibrated the (2 + 1) REMPI–TOF/MS detection scheme for H_2, HD, and D_2 against a thermal effusive source. Vibrational and rotational correction factors have been obtained for 102 rovibrational levels for $v'' = 0,1$, and 2 and J'' ranging from 0 to 17. These correction factors allow ion signals to be converted into relative quantum-state populations without relying on any theoretical description of the (2 + 1) REMPI process. For low J'' levels, the rotational correction factors are close to unity. However, vibrational correction factors vary significantly with v'' and are sensitive to saturation and to the presence of dissociative channels.

We can compare these correction factors to those obtained from a theoretical calculation of the two-photon transition moments.[21] Most experimental and theoretical correction factors agree within their combined uncertainties. Exceptions occur for high J'' levels in which the $(v'_E = 0,\ J')$ wave function has appreciable delocalization, which is caused by tunneling from the E well into the F well of this double-minimum potential. This behavior suggests that theoretical correction factors can be used reliably when experimental ones are unavailable for (v',J') levels in which delocalization is unimportant, in particular, $J'' < 11$ in H_2.

ACKNOWLEDGMENTS

We are grateful to M. Gutierrez for his skillful assistance in the construction of the oven and to A. C. Kummel and G. O. Sitz for many useful discussions about the design. We thank Y. T. Lee and R. E. Continetti for the HD gas used in the experiment. D.A.V.K. gratefully acknowledges a GAANN graduate fellowship from the U.S. Department of Education. This project is supported by the National Science Foundation under Grant No. NSF CHE 90-07939.

[1] J. W. Nibler, J. R. McDonald, and A. B. Harvey, Opt. Commun. **18**, 371 (1976).
[2] M. Pealat, J. P. E. Taran, J. Taillet, M. Bacal, and A. M. Brunteau, J. Appl. Phys. **52**, 2687 (1981); M. Pealat, D. Debarre, J. M. Marie, J. P. E. Taran, A. Tramer, and C. B. Moore, Chem. Phys. Lett. **98**, 299 (1983).
[3] C. R. Quick, Jr., and D. S. Moore, J. Chem. Phys. **79**, 759 (1983).
[4] D. P. Gerrity and J. J. Valentini, J. Chem. Phys. **79**, 5202 (1983); **81**, 1298 (1984); D. K. Veirs, G. M. Rosenblatt, and J. J. Valentini, *ibid.* **83**, 1605 (1985).
[5] A. Slenczka, G. Marowsky, and M. Vodegel, Appl. Phys. B **47**, 41 (1988).
[6] T. Dreier and J. Wolfrum, Int. J. Chem. Kin. **18**, 919 (1986); J. Arnold, T. Dreier, and D. W. Chandler, Chem. Phys. **133**, 123 (1989).
[7] E. E. Marinero, C. T. Rettner, R. N. Zare, and A. H. Kung, Chem. Phys. Lett. **95**, 486 (1983).
[8] F. J. Northrup, J. C. Polanyi, S. C. Wallace, and J. M. Williamson, Chem. Phys. Lett. **105**, 34 (1984).
[9] H. Zacharias and R. David, Chem. Phys. Lett. **115**, 205 (1985); L. Schröter, H. Zacharias, and R. David, Appl. Phys. A **41**, 95 (1986); W. Meier, G. Ahlers, and H. Zacharias, J. Chem. Phys. **85**, 2599 (1986).
[10] C. D. Pibel, K. L. Carleton, and C. B. Moore, J. Chem. Phys. **93**, 323 (1990); C. D. Pibel and C. B. Moore, *ibid.* **93**, 4804 (1990).
[11] E. E. Marinero, C. T. Rettner, and R. N. Zare, Phys. Rev. Lett. **48**, 1323 (1982); E. E. Marinero, R. Vasudev, and R. N. Zare, J. Chem. Phys. **78**, 692 (1983).
[12] H. Rottke and K. H. Welge, Chem. Phys. Lett. **99**, 456 (1983); W. Meier, H. Rottke, H. Zacharias, and K. H. Welge, J. Chem. Phys. **83**, 4360 (1985); L. Schröter, G. Ahlers, H. Zacharias, and R. David, J. Electron Spectrosc. Relat. Phenom. **45**, 403 (1987); H. Zacharias, Appl. Phys. A **47**, 37 (1988); L. Schröter, H. Zacharias, and R. David, Phys. Rev. Lett. **62**, 571 (1989).
[13] A. H. Kung, T. Trickl, N. A. Gershenfeld, and Y. T. Lee, Chem. Phys. Lett. **144**, 427 (1988).
[14] E. E. Marinero, C. T. Rettner, and R. N. Zare, J. Chem. Phys. **80**, 4141 (1984); R. S. Blake, K.-D. Rinnen, D. A. V. Kliner, and R. N. Zare, Chem. Phys. Lett. **153**, 365 (1988); K.-D. Rinnen, D. A. V. Kliner, R. S. Blake, and R. N. Zare, *ibid.* **153**, 371 (1988); K.-D. Rinnen, D. A. V. Kliner, and R. N. Zare, J. Chem. Phys. **91**, 7514 (1989).
[15] D. A. V. Kliner and R. N. Zare, J. Chem. Phys. **92**, 2107 (1990); D. A. V. Kliner, K.-D. Rinnen, and R. N. Zare, Chem. Phys. Lett. **166**, 107 (1990).
[16] D. A. V. Kliner, D. E. Adelman, and R. N. Zare, J. Chem. Phys. **94**, 1069 (1991).
[17] D. A. V. Kliner, K.-D. Rinnen, and R. N. Zare, J. Chem. Phys. **90**, 4625 (1989); K.-D. Rinnen, D. A. V. Kliner, M. A. Buntine, and R. N. Zare, Chem. Phys. Lett. **169**, 365 (1990).
[18] D. W. Chandler and R. L. Farrow, J. Chem. Phys. **85**, 810 (1986); R. L. Farrow and D. W. Chandler, *ibid.* **89**, 1994 (1988).
[19] G. D. Kubiak, G. O. Sitz, and R. N. Zare, J. Chem. Phys. **81**, 6397 (1984); **83**, 2538 (1985); J. Vac. Sci. Technol. A **3**, 1649 (1985).
[20] D. J. Kliger and C. K. Rhodes, Phys. Rev. Lett. **40**, 309 (1978); D. J. Kliger, J. Bokor, and C. K. Rhodes, Phys. Rev. A **21**, 607 (1980).
[21] W. M. Huo, K.-D. Rinnen, and R. N. Zare, J. Chem. Phys. **95**, 205 (1991).
[22] K.-D. Rinnen, D. A. V. Kliner, R. N. Zare, and W. M. Huo, Israel J. Chem. **29**, 369 (1989).
[23] K.-D. Rinnen, D. A. V. Kliner, and R. N. Zare, J. Chem. Phys. **91**, 7514 (1989).
[24] K.-D. Rinnen, D. A. V. Kliner, R. S. Blake, and R. N. Zare, Rev. Sci. Instrum. **60**, 717 (1989).
[25] The barium borate crystals were supplied by R. S. Feigelson and R. K. Route and grown as part of a research program sponsored in part by the Army Research Office, Contract No. DAAL03-86-K-0129, and in part by the NSF/MRL Program through the Center for Materials Research, Stanford University.
[26] R. S. Blake, Ph.D. thesis, Department of Chemistry, Stanford University, 1988.
[27] C. Barroux and M. M. Audibart, Chem. Phys. Lett. **66**, 483 (1979).
[28] J. E. Pollard, D. J. Trevor, Y. T. Lee, and D. A. Shirley, J. Chem. Phys. **77**, 4818 (1982).
[29] E. A. Rohlfing, H. Rabitz, J. Gelfand, and R. B. Miles, J. Chem. Phys. **81**, 820 (1984).
[30] K. Kerm, R. David, and G. Comsa, J. Chem. Phys. **82**, 5673 (1985).
[31] P. W. Atkins, *Physical Chemistry* (Freeman, San Francisco, 1982).
[32] J. H. Kiefer and R. W. Lutz, J. Chem. Phys. **44**, 668 (1966).
[33] M.-M. Audibart, C. Joffrin, and J. Ducuing, Chem. Phys. Lett. **25**, 158 (1974).
[34] M.-M. Audibart, R. Vilaseca, J. Lukasik, and J. Ducuing, Chem. Phys. Lett. **31**, 232 (1975).
[35] J. E. Dove and H. Teitelbaum, Chem. Phys. **6**, 1431 (1974).
[36] T. G. Kreutz, J. Gelfand, R. B. Miles, and H. Rabitz, Chem. Phys. **124**, 359 (1988).
[37] J. B. Calvert, J. Chem. Phys. **56**, 5071 (1972).
[38] H. Teitelbaum, Chem. Phys. Lett. **106**, 69 (1984).
[39] J. H. Kiefer and R. W. Lutz, J. Chem. Phys. **44**, 658 (1966).
[40] J. Lukasik and J. Ducuing, J. Chem. Phys. **60**, 331 (1974).
[41] J. Lukasik and J. Ducuing, Chem. Phys. Lett. **27**, 203 (1974).
[42] K. P. Huber and G. Herzberg, *Molecular Spectra and Molecular Structure. IV. Constants of Diatomic Molecules* (Van Nostrand Reinhold, New York, 1979).
[43] A particularly useful dye mix under our experimental conditions was oscillator = 105 mg/l DCM, 41 mg/l R640 and amplifier = 8.0 mg/l DCM, 12 mg/l R640 in methanol. This covers 602–665 nm, corresponding to $v'' = 0$, 1, and most of 2 for all three gases.
[44] K.-D. Rinnen, D. A. V. Kliner, R. S. Blake, and R. N. Zare, Chem. Phys. Lett. **153**, 371 (1988).
[45] D. Normand, C. Cornaggia, and J. Morellec, J. Phys. B **19**, 2881 (1986).
[46] J. D. Buck, D. H. Parker, and D. W. Chandler, J. Phys. Chem. **92**, 3701 (1988).
[47] M. A. Buntine, D. P. Baldwin, and D. W. Chandler (private communication).
[48] E. Y. Xu, H. Helm, and R. Kachru, Phys. Rev. A **39**, 3979 (1989).

[49] S. L. Anderson, G. D. Kubiak, and R. N. Zare, Chem. Phys. Lett. **105**, 22 (1984).
[50] N. Bjerre, R. Kachru, and H. Helm, Phys. Rev. A **31**, 1206 (1985).
[51] C. Cornaggia, J. Morellec, and D. Normand, J. Phys. B **18**, L501 (1985).
[52] C. Cornaggia, J. Morellec, and D. Normand, Phys. Rev. A **34**, 207 (1986).
[53] H. Rudolph, D. L. Lynch, S. N. Dixit, and V. McKoy, J. Chem. Phys. **86**, 1748 (1987).
[54] C. Cornaggia, A. Giusti-Suzor, and Ch. Jungen, J. Chem. Phys. **87**, 3934 (1987).
[55] N. Sen, K. Rai Dastidar, and T. K. Rai Dastidar, Phys. Rev. A **38**, 841 (1988).
[56] J. D. Buck, D. C. Robie, A. P. Hickman, D. J. Bamford, and W. K. Bischel, Phys. Rev. A **39**, 3932 (1989).
[57] E. Xu, A. P. Hickman, R. Kachru, T. Tsuboi, and H. Helm, Phys. Rev. A **40**, 7031 (1989).
[58] W. T. Hill III, B. P. Turner, S. Yang, J. Zhu, and D. L. Hatten, Phys. Rev. A **43**, 3668 (1991).
[59] W. M. Huo (unpublished results).
[60] B. Peart and K. T. Dolder, J. Phys. B **8**, 1570 (1975).
[61] K. Nakashima, H. Takagi, and H. Nakamura, J. Chem. Phys. **86**, 726 (1987).
[62] H. Hus, F. Yousif, C. Noren, A. Sen, and J. B. A. Mitchell, Phys. Rev. Lett. **60**, 1006 (1988).
[63] P. Quadrelli, K. Dressler, and L. Wolniewicz, J. Chem. Phys. **93**, 4958 (1990).
[64] D. C. Hanna, M. A. Yuratich, and D. Cotter, *Nonlinear Optics of Free Atoms and Molecules* (Springer, New York, 1979), p. 174.